Spectral response of few important textural variants of chromitite and its potential in estimating relative grades of chromitite – a case study for chromitite of Nuggihalli Schist Belt, India

Arindam Guha[1,*], Biswajit Ghosh[2], Sukanya Chaudhury[2], Komal Rani[1] and K. Vinod Kumar[1]

[1]Geosciences Group, National Remote Sensing Centre, Indian Space Research Organization, Balanagar, Hyderabad 500 625, India
[2]Department of Geology, University of Calcutta, 35 Ballygunge Circular Road, Kolkata 700 019, India

We have collected, processed and analysed the reflectance spectra of representative chromitite samples of spot type, clot type and disseminated type textural variants to understand the diagnostic spectral features of each of these samples. We have found that the reflectance spectrum of each textural variant is distinct from the spectra of other variants despite having few common absorption features. Spectral features of chromitite samples are governed by the spectra of two dominant minerals, chromite and chlorite. Spectral features of chromitite at 550 nm and 1100 nm are governed by electronic transition process in Fe^{3+} and crystal field effect in Fe^{2+} ions present in chromite structure respectively. On the other hand, spectral features at 1400 nm, 1900 nm and 2300 nm are related to the vibration of O–H, H–OH and metal hydroxide bonds in chlorite. Amongst these features, the spectral feature at 1100 nm (due to Fe^{2+} in chromite grains) is common to all three major textural varieties of chromitite samples studied here. Electron probe micro analysis (EPMA) data of chromite and chlorite grains of each texture are used to relate the presence and abundance of Fe^{2+} (in chromite grains) with absorption feature. Width of the 1100 nm feature has a correlation value 0.95, while depth of the same feature has a correlation value 0.94 with the abundance of chromite mineral estimated using modal analysis of chromite samples. Therefore, spectrometric parameter of 1100 nm spectral feature of chromitite can be used as proxy for estimating modal abundance of chromite in chromitite samples after estimating deposit specific correlation coefficient.

Keywords: Chromitite, electronic processes, modal analysis, spectral feature, texture, vibrational processes.

REFLECTANCE spectroscopy deals with reflectance variations across spectral domains. Reflectance spectra of terrain elements (rocks) are characterized by absorptions with local reflectance maxima[1–3]. These features are known as spectral features or absorption features[3]. Spectral features of rocks and minerals collected from remote platforms are key for spatial mapping of rocks and minerals as spectroscopy-based delineation is not affected by sensor to target distance[4–6]. In general, spectral features of rocks are analysed based on the mineralogically sensitive diagnostic spectral features identified on the basis of supporting data on quantitative mineralogy[3,4]. In terms of wavelength, spectral profiles of rocks are related to but distinct from the spectral features of dominant constituent minerals[1–3,7,8]. Rock spectra are the result of mixing of the spectra of dominant constituent minerals, which have diagnostic spectral features within specific spectral domain[3,9,10]. Besides the texture of the rock and instantaneous field of view (IFOV) of spectroradiometer, other measurement parameters (spectral bandwidth, spectral resolution of the instrument/spectrometer, angle between illuminator and measurement optics) also have influences in modifying depth, width and overall shape of the absorption features of rock spectra[3,7,11]. Spectral characterization of chromitite samples associated with other ultramafic host rocks (e.g. dunite, pyroxenite, peridotite, etc.) is an interesting aspect to study and it has its utility in chromite exploration. Spectral remote sensing of ophiolites demonstrated the utility of absorption features of reflectance spectra to recognize or spatially delineate ultramafic rocks[12–17]. However, spectral characterization of chromitite samples with variable concentrations of chromite and associated constituent minerals has not been attempted earlier. In this study, spot type, clot type and disseminated type[18] chromitites from the Nuggihalli greenstone belt (Karnataka, India) have been spectrally characterized. Each of the chromitite types has a specific range of abundances of constituent minerals with their characteristic mutual arrangements in their rock fabric.

*For correspondence. (e-mail: guha_arindam@yahoo.com)

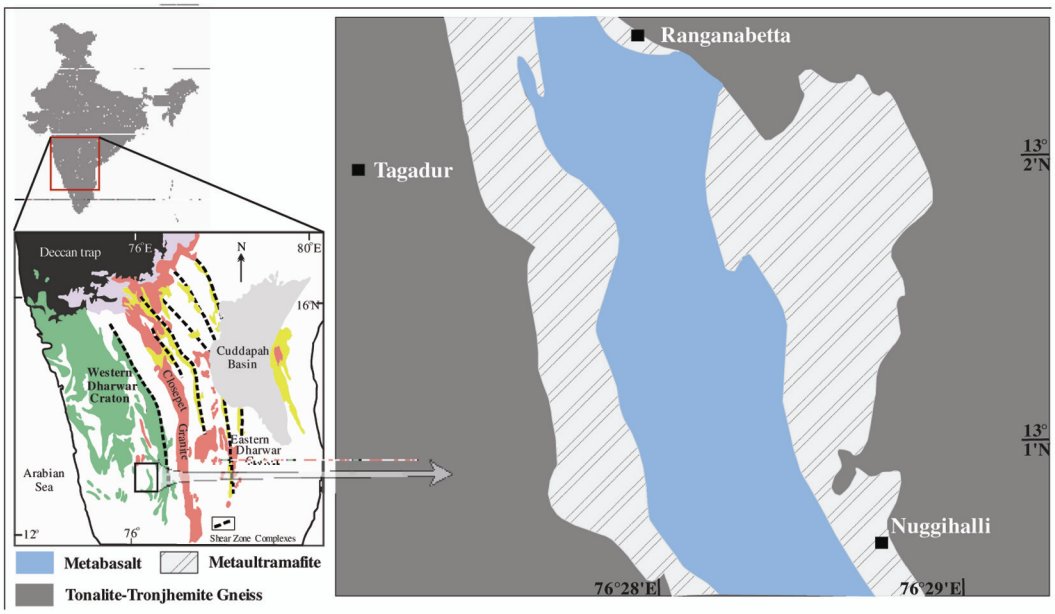

Figure 1. Generalized geological map of Nuggihalli greenstone belt (modified after Jafri *et al.*[38]) with inset geopolitical map of India and geological map of southern India.

Different mutual arrangements of minerals in a rock fabric allow different combinations of dominant constituent minerals to occur within the diameter of sampling area (proportionate to IFOV) to be used for collecting reflectance spectra. Thus variable spectral responses can be received from samples of different textures having variable chromite content. Therefore, from an economic point of view, it is imperative to understand how reflectance spectra of the chromitites can be used to estimate the mineralogical abundances of different textural variants. Reflectance spectroscopy, in addition to being non-destructive, provides a rapid assessment of the mineralogical composition of rocks, as the sample preparation process is simple and fast[3]. In reflectance spectroscopy, rock samples are generally cut into regular sizes keeping natural surface exposures intact for spectroscopic study. The samples are illuminated by halogen light as laboratory grade halogen lamps behave as near black bodies and have irradiance curves similar to sunlight[19]. Reflectance spectroscopy has been widely used to characterize the minerals and rocks on Earth and other planets[3,4,20,21].

This study has attempted to evaluate the potential of reflectance spectroscopy in estimating the abundance of chromite in chromitite rock samples of different textures. A similar study is absent in the literature although spectra of chromite were studied with reference to spinel reflectance spectra[22].

Study area and geology

The study area, the Nuggihalli greenstone belt, is located in the central north of Karnataka, one of the southern states of India (Figure 1). This linear ultramafic–mafic belt is known for stratiform chromitite deposit and occurs within the oldest greenstone belt within the vast gneissic country of the Western Dharwar Craton[23] (Figure 1). The rocks in the Nuggihalli belt belong to the Sargur Group[18], which occurs as enclaves within the Tonalite–Trondjhemite–Granodiorite Gneisses (TTG) and dominantly consists of metamorphosed conformable volcanic rocks (e.g. komatiite and komatiitic basalt) and metasedimentary rocks, both now occurring as schist. Several layered intrusive plutonic bodies consisting of ultramafic rocks (metamorphosed to serpentine-chlorite schist, serpentine-talc schist) and pyroxenites (metamorphosed to talc-chlorite-tremolite schist), gabbro and anorthosite are present within these schistose rocks[24,25]. Chromitite exposures occur as bands (centimetre scale) and lenses hosted within the meta-ultramafic rocks[26]. Many chromitite exposures in the study area have been excavated due to extensive open cast mining activity. These exposures can be targeted using earth observation sensors capable of recording detailed spectroscopic data with high spectral resolution. Representative photographs of chromitite exposures are given in Figure 2. In these figures, chromitites are seen as lenses (Figure 2 *a*, *d*), bands (Figure 2 *b*) and also as massive blocks (Figure 2 *c*).

Methodology

Field work

Field work was carried out to understand the geological set-up and mode of occurrence of chromitites in the study

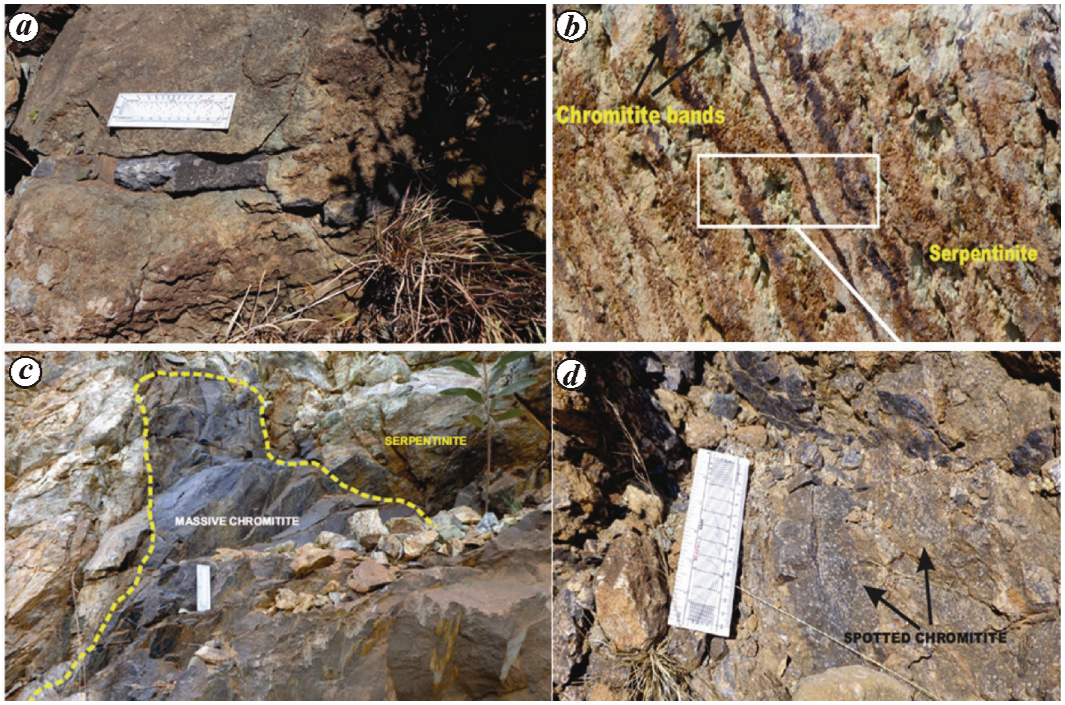

Figure 2. Spatial association of chromitite and serpentine rich meta-ultramafite in Nuggihalli-schist belt. ***a***, Chromitite (dark coloured) lense within serpentinized metaultramafite. ***b***, Chromitite band within serpentine rich meta-ultramafite. ***c***, Massive chromitite block within Ranganbetta mine. ***d***, Disseminated textured (spotted and lensoid) chromitite in Jambur mine.

area. During field work, samples were collected from surface exposures of chromitite within open cast mines and also from natural exposures around mines. Chromitite sample which had megascopically distinct textural variations only were collected. Large samples were collected for each textural variant of chromitite. Samples were further fragmented into two additional replicas, one each for spectral data collection and mineralogical/petrographical analysis. Samples used for petrographical analysis were consequently used for mineral-chemical studies (electron probe micro-analysis) to estimate oxide abundances in single chromitite and chlorite mineral grains of representative samples of each textural variant and also to understand the distribution of Fe^{3+} and Fe^{2+} in these samples.

Mineralogical/petrographical analysis

Detailed petrography including modal analysis of chromitite samples was carried out to delineate different types of textures of chromitite samples and also to estimate the relative abundance of constituent minerals in each textural variant. Depending on the mutual arrangements among constituent minerals, chromitites display a variety of textures under microscope. These are disseminated, spotted and clot textures (Figure 3). In the spot textured chromitite, chromite minerals constitute mesh or spot-like fabric. In clot texture, fine euhedral chromite grains are bound together with coarse chromite grains and appear as bands or clots. In disseminated textured chromitite, chromite grains are randomly scattered in chloritic mass. Chromite concentrations were highest in clot type texture and lowest in disseminated texture. It was intermediate in range in spot type texture (Table 1). Chromite modal abundance was variable broadly within the range of 50–75% in different chromitite samples of three distinct textures (Table 1). Modal abundances of each constituent mineral were estimated from rock thin sections, which have also been used to analyse textures of different samples. Modal analysis was accomplished on standard petrographic microscope with a manual mechanical stage with mm-graduated x–y stage translation that controlled the movement of the thin section. In this regard, mineral abundance was estimated from evenly spaced data point-intercepts along selected parallel traverse lines cutting across the entire extent of the thin section. Spacing between adjacent lines was kept at 0.5 mm (y parameter) and measurement points were kept at 0.25 mm (x parameter) interval along each line for identification and quantification of the mineral under the ocular of the microscope. The measurement was made on both the thin sections prepared parallel and across the rock fabric and the counting for each mineral was averaged out. Modal analysis provided the volumetric abundance of each constituent mineral in chromitite samples. The results of modal analysis of representative samples of chromitites with varying textures are provided in Table 1. The textural

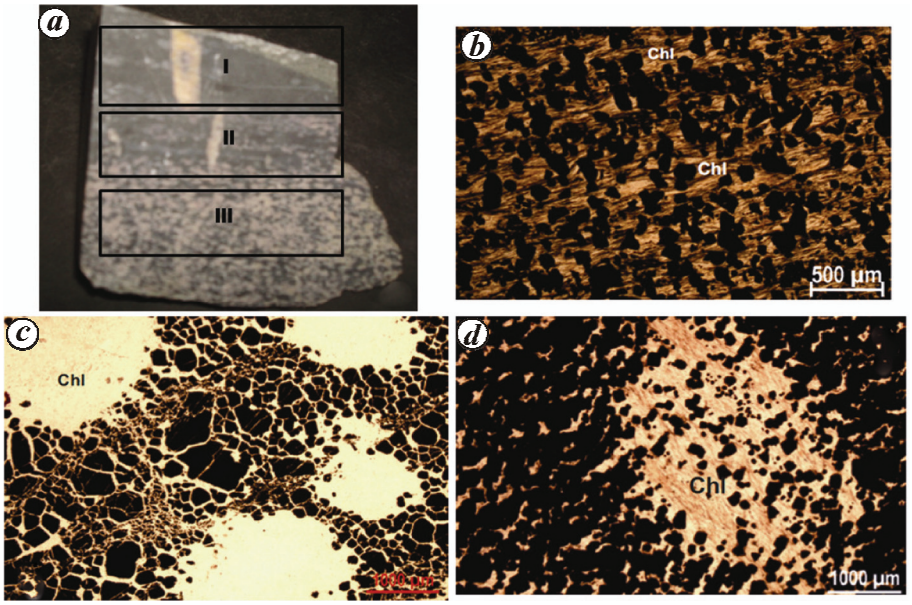

Figure 3. ***a***, Rock sample showing clot (I), spot (II) and disseminated (III) textured chromitite. Photomicrograph of disseminated (***b***), spot (***c***) and clot (***d***) textured chromitite.

Table 1. Modal analysis of representative samples of chromitite (for each dominant textural variant)

		Modal abundances				
Rock	Mineral	Chromitite_dsm_01	Chromitite_dsm_04	Chromitite_dsm_05	Chromitite_dsm_02	Chromitite_dsm_03
Chromitite (disseminated texture)	Chlorite	30%	34.5%	33%	31%	31%
	Chromite	51%	53.5%	55.3%	52%	52%
	Serpentine	19%	12%	11.7%	17%	17%
Chromitite (spotted texture)		Chromitite_ spot_05	Chromitite_ spot_04	Chromitite_ spot_01	Chromitite_ spot_03	Chromitite_ spot_02
	Chromite	65.5%	63%	60%	62.6%	61%
	Chlorite	27%	25.2%	29%	30.3%	29%
	Serpentine	7.5%	11.8%	11%	7.1%	10%
Chromitite (clot texture)		Chromitite_ clot 1_05	Chromitite_ clot_04	Chromitite_ clot_03	Chromitite_ clot_02	Chromitite_ clot_05
	Chromite	70.5%	74.8%	73%	71.9%	76%
	Chlorite	20%	19%	17.8%	20.2%	17%
	Serpentine	9.5%	6.2%	9.2%	7.9%	7%

variations of chromitite were well discernible in hand specimens as observed in the thin sections (Figure 3). To correlate the Fe^{2+}/Fe^{3+} ratio of chromite minerals in chromitite samples with their spectral response, the above ratio was determined from mineral chemistry analysis (EPMA) of polished thin sections of the chromitite samples (Table 2). This analysis was performed at the Central Petrological Laboratory, Geological Survey of India, Kolkata with a CAMECA SX100 EPMA machine at an accelerating voltage of 15 kV and a beam current of 12 nA using 1 µm diameter beam. The Fe^{2+}–Fe^{3+} partitioning of chromite was calculated based on the charge balance equation[27]. Tetrahedral or octahedral coordination of Fe^{2+} and oxidation state of Fe in the mineral structure influence the spectral response of Fe bearing minerals within the spectral domain of 350–1150 nm (ref. 28).

Collection of reflectance spectra

Spectral observations were collected using the Field Spec 3© spectroradiometer, which has three detectors within the spectral domain of 350–2500 nm. The silicon detector collects reflected energy within the spectral domain of 350–1000 nm, whereas two indium–gallium–arsenide (InGaAS) detectors collect reflected energy within the spectral domain of 1000–1800 nm and 1800–2500 nm respectively[19]. Rectangular samples with sizes of approximately 4–5 inches were suitable for properly placing the sample under the fore optics of the spectroradiometer.

Table 2. Electron probe microanalyses of representative spots on a single chromite grain of selected samples of chromitites of each variant. Table shows the relative enrichment of Fe^{3+}

	(Chromitite sample 1)-clot type	(Chromitite sample 2)-spot type	(Chromitite sample 3)-disseminated type	(Chromitite sample 1)	(Chromitite sample 2)	(Chromitite sample 3)
Minerals	Chromite	Chromite	Chromite	Chlorite	Chlorite	Chlorite
SiO_2	–	–	–	33.42	34.46	33.24
TiO_2	1.01	0.99	0.80	0.03	–	0.01
Al_2O_3	0.34	0.36	0.34	12.59	11.99	12.77
Cr_2O_3	35.41	32.79	34.92	1.79	1.03	1.50
Fe_2O_3	30.81	33.23	31.57	–	–	–
FeO	30.62	29.81	30.81	5.96	5.59	6.51
MnO	1.05	1.63	0.82	0.11	0.06	0.14
NiO	0.25	0.29	0.13	0.14	0.17	0.17
MgO	0.41	0.42	0.35	33.27	33.8	33.27
Total	99.90	99.52	99.74	87.31	86.2	87.25
Oxygen	4	4	4	28	28	28
Si	–	–	–	6.395	6.574	6.36
Ti	0.029	0.028	0.023	0.000	0.000	–
Al	0.015	0.016	0.015	2.844	2.698	2.892
Cr	1.055	0.981	1.042	0.271	0.155	0.23
Fe^{3+}	0.873	0.946	0.807	–	–	–
Fe^{2+}	0.965	0.943	0.973	0.990	0.897	1.050
Mn	0.033	0.052	0.026	0.018	0.010	0.020
Ni	0.008	0.009	0.004	0.022	0.026	0.030
Mg	0.023	0.024	0.020	9.490	9.613	9.493
Total	3	3	3	20	20	20

Tungsten–argon halogen lamp fused with silica was used to irradiate samples as the lamp is known for stable irradiance within the spectral domain of 350–2500 nm (ref. 19). The light source was fixed at 45° relative to the samples. This angle is known as phase angle[7,29,30]. Fixing of the phase angle was essential to record the reflected energy resulting from volume scattering at the surface of the rock sample[7,29]. The reflectance spectra were derived by normalizing radiance reflected from the samples with respect to the radiance reflected by a lambertian reflector panel, known as calibration panel or white panel in the field of spectroscopy[29]. Spectralon, an optical graded compound, was used as the calibration panel to derive reflectance[30–33]. Spectral data were collected for 3–4 spots of each sample. Spectra of each spot, in turn, were deduced by averaging 30 spectral observations. Mean spectra of rock samples were derived by averaging spectral profiles of all spots of that sample (Figure 4 *a*).

Rock spectra of chromitite samples thus collected were the integrated product of the combined spectral response of constituent minerals of the samples. Therefore, reference reflectance spectra of minerals were taken from the spectral library of United States Geological Survey (USGS) to analyse the mineralogical significance of each absorption feature of samples of each textural variant (Figure 4 *b* and *c*). The role of different controlling parameters responsible for shaping the rock spectra (phase angle of measurement, sample to sensor distance, grain size of sample) and the mineralogical significance of spectral features have been studied earlier[2,6–9,16,33]. Previous studies have also shown that wavelength positions of absorption features are sensitive to mineralogy, while absolute reflectance values of spectral profiles are affected by grain size, intimate mixing and other spectral measurement parameters of reflectance spectra[3,7,11]. In order to calculate the quantitative parameters of the spectral feature of the chromitite sample, we normalized each spectra of the chromitite sample with respect to the 'continuum' of the same spectra (Figure 5 *a* and *b*). This was done for all the samples representing intra- and inter-textural spectral variation (Figure 6). Continuum is an imaginary line joining points of the mean back ground reflectance of the spectral curve[34–36] and it is also schematically shown (Figure 5 *a* and *b*). It is important to note that the continuum removal process was an essential requirement for comparing the spectra of one mineral with the other based on the quantitative parameters of absorption features[3,35,36]. Width, one of the important quantitative spectrometric parameters, was derived from continuum removed spectra by calculating the difference in wavelength between two shoulders (prominent reflectance peak occurring either side of spectral feature or absorption minima). Depth of the absorption feature was derived based on calculating differences in normalized reflectance between the continuum and minimum reflectance point (i.e. absorption minima) of the absorption feature.

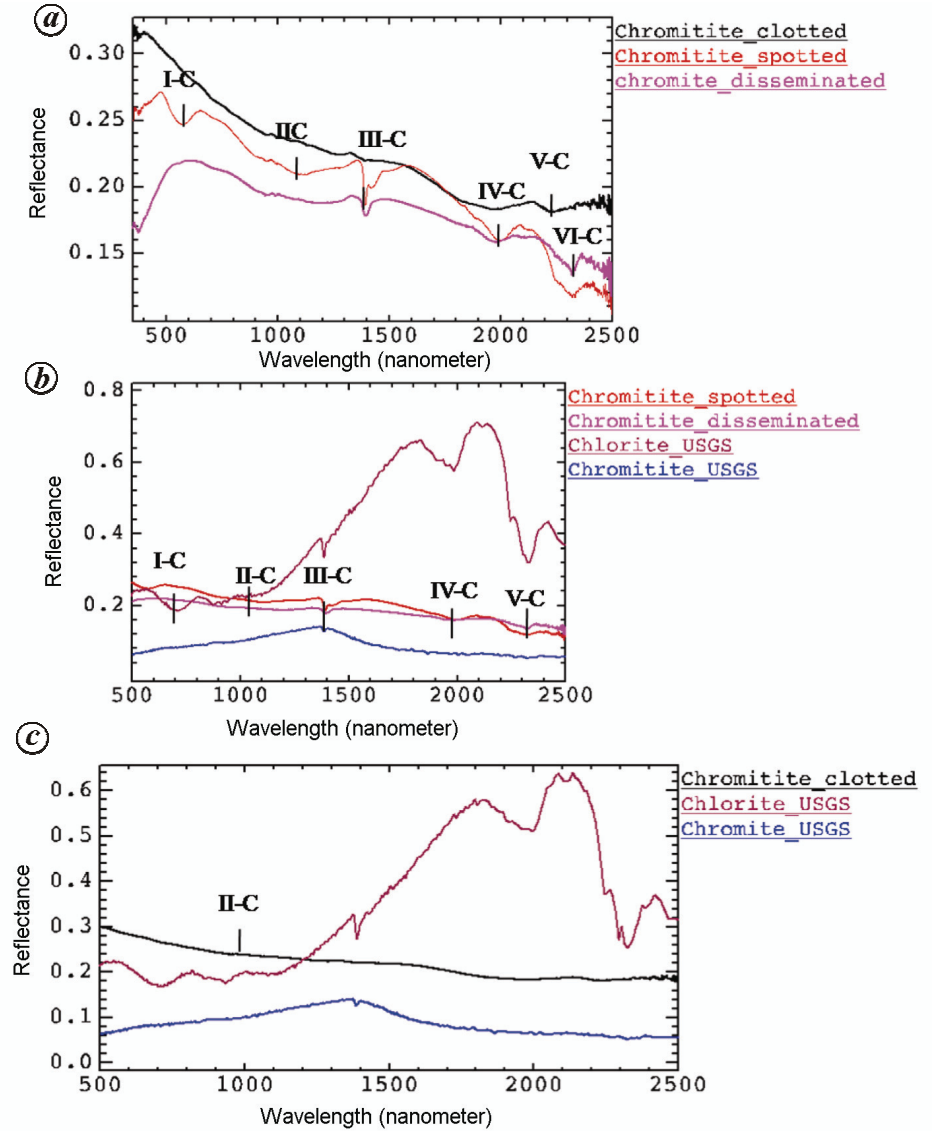

Figure 4. ***a***, Spectral profiles of different chromitite samples of distinct textural variants. ***b***, Spectral profiles of chromitite samples of disseminated and spot type texture with spectra of major constituent minerals of rocks (USGS lab). ***c***, Spectral profiles of chromitite of clot type texture with spectra of major constituent minerals of rocks (USGS lab). Absorption or spectral features are labelled as I–C to V–C.

Continuum removed reflectance spectra of powdered samples of all the textural variants of chromitites were used to calculate width and depth of diagnostic absorption features for correlating them with modal abundance of chromite (Figure 5 *b*), while reflectance spectra of consolidated samples were used to identify intra-texture and inter-texture variations in reflectance spectra of chromite samples (Figures 4 and 6). The relation between the spectra of rock samples (with original fabric intact) and its pulverized counterpart has been well discussed in the literature[7]. For making pulverized samples, all 15 samples were sieved with a mesh of size range 149–250 μm to make the grain size and the intimate mixing factors invariant on the geometric/spectrometric parameters of diagnostic spectral features, like depth and width[3].

Results and discussion

In this study, we identified three different textural variants of chromitites (Figure 3). In disseminated type chromitite, chromites were almost homogeneously distributed in the rock sample (Figure 3 *b*). On the other hand, in spot type chromitite, chromitite bands were found to segregate as isolated patches (Figure 3 *c*). In the clot type, distinct cumulates or bands of chromite minerals were identified. These dense bands of chromite were separated from each other by thin lenses of chlorite (Figure 3 *d*). As seen from the spatial disposition of minerals in each texture, relative abundances of the two major minerals (i.e. chromite and chlorite) were different in each textural variant (Figure 3 *b* to *d* and Table 1). Therefore,

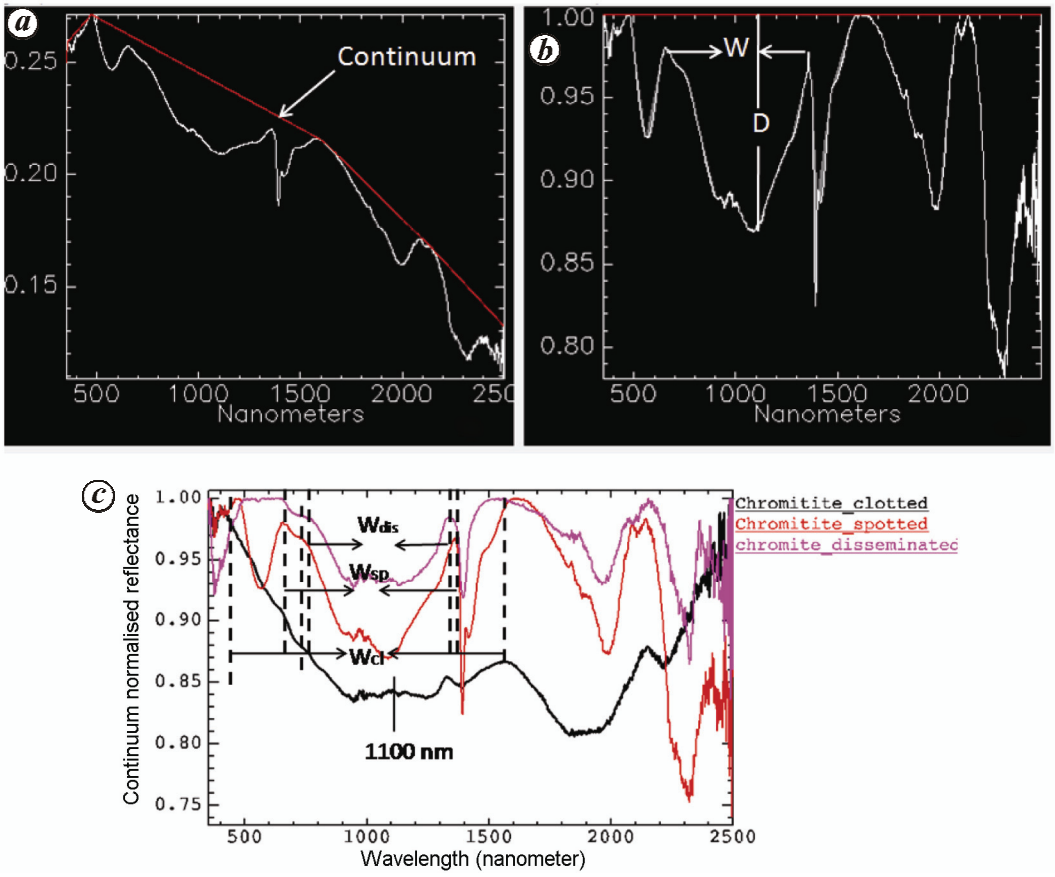

Figure 5. ***a***, Schematic diagram showing continuum of a spectral profile. ***b***, Schematic diagram illustrating width (w) and depth (d) of a spectral profile. ***c***, Continuum removed spectra of representative samples of disseminated type, clot and spot type chromitite. The width of 1100 nm spectral feature of disseminated (W_{dis}), clot (W_{cl}) and spo (W_{sp}) is also shown.

each textural variant was characterized with distinct reflectance spectra with few absorption features (Figure 4 *a*). While comparing spectra of spot and disseminated type chromitite samples, we found that spot type chromitite had absorption minima at around 550 nm (*I–C*), which was distinct with respect to the spectral feature of disseminated samples (Figure 4 *a*). We also observed that the spectra of clot type chromitite were distinct from that of disseminated and spot type chromitite samples by the absence of the 2300 nm (VI–C) feature and the presence of a 2200 nm feature (V–C) (Figure 4 *a*). The spectral feature at 2200 nm (V–C) was earlier reported in the spectra of Fe rich chromite in the literature[15]. The spectral features at 1100 nm (II–C), 1400 nm (III–C), 1800–1900 nm (IV–C) and 2300 nm were common to both spot and disseminated texture chromitite but absorption minima of spot type chromitite at 550 nm (I–C) was absent in the disseminated type counterpart (Figure 4 *b*). The atomic processes responsible for imprinting these features are summarized in Table 3 (refs 12, 15, 17, 37).

Spectra of chromitite samples were influenced by chlorite for the absorption features at 1400, 1900 and 2300 nm (marked as III–C, IV–C and VI–C in Figure 4 *b*)[5,38]. But the spectral feature around 1100 nm (II–C) was influenced by the presence of Fe^{2+} in chromite (Figure 4 *b* and Table 3). Further, the spectra of clot textured chromitite had a sharp fall in reflectance from 450 to 500 nm and had broad reflectance minima around 1100 nm (Figure 4 *c*). The absorption feature at 1100 nm was enhanced in continuum removed spectra of chromitite samples of different textures with their spectrometric parameters such as width and depth (Figure 5 *c*). It was observed that the continuum removed spectral feature of clot type chromitite sample at 1100 nm was characterized with asymmetric shape (due to the presence of shoulder (S) of the absorption feature at different distances on either side of the absorption minima along the wavelength axis) with a wider base of absorption minima. However, the same absorption feature was narrow and relatively symmetric for clot and disseminated type chromitite samples (Figures 6 *a–c*). Wider base of reflectance minima in samples of clot type chromitite was attributed to the coalescence of two absorption features at 900 and 1100 nm due to the presence of Fe^{2+} in tetrahedral and octahedral places respectively[12,13]. This feature further extended towards lower wavelength due to possible presence of Fe^{3+} feature at 550 nm in chromite mineral in the clot type variant of chromitite (Figure 6 *a*).

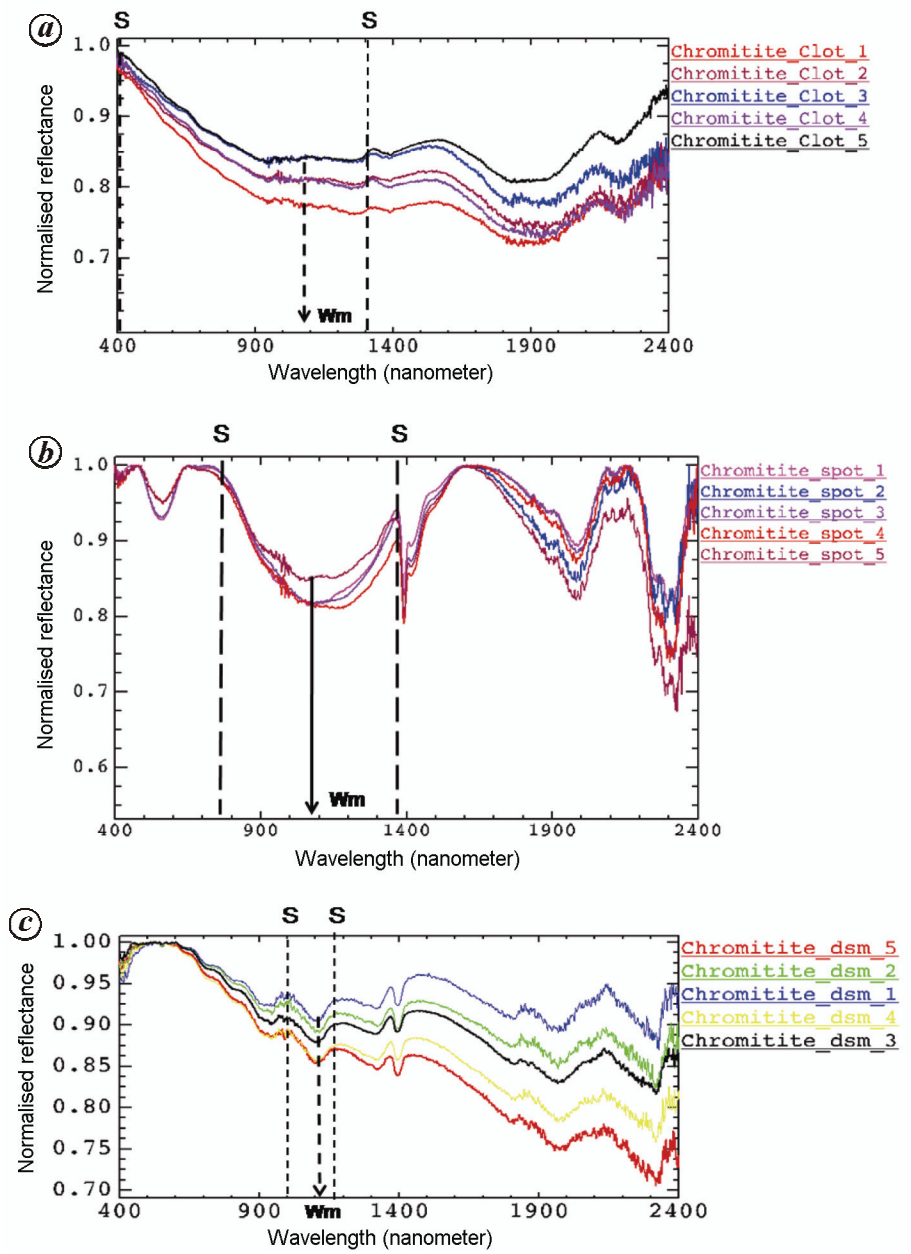

Figure 6. ***a***, Spectral profiles of selected five samples of clot type chromitite. In these samples, chromite contents increased from sample chromitite_clot_1 to chromitite_clot_5. ***b***, Spectral profiles of selected five samples of spotted type chromitite. In these samples, chromite contents increased from sample chromitite_spot_1 to chromitite_spot_5. ***c***, Spectral profiles of selected five samples of disseminated type chromitite. In these samples, chromite sample contents increased from sample chromitite_dsm_1 to chromitite_dsm_5. Refer Table 1 to find the modal abundance of chromite in each sample. In these figures, shoulder (S) and wavelength of absorption minima (Wm) of the absorption figures are shown.

While comparing continuum removed spectra of chromitite samples of different textures, we found that the spectral feature at 1100 nm was common to the three variants of chromitite, but the width and depth of the spectral feature were variable in different textural varieties but similar (i.e. very close with slight variation) for samples of the same texture (Figures 5 *c* and 6 *a–c*). This was attributed due to contrast in the variation of chromite content (5–7%) among the samples of the same textural variant (5–7%) and different textural variations (20–25%) (Table 1). Depth and width of this feature were found maximum for clot-type chromitite spectra, whereas these parameters were minimum in the spectra of disseminated chromitite samples (Figure 5 *c*). We made an attempt to relate the width and depth of the absorption feature at 1100 nm with the abundance of chromite (modal abundance) in

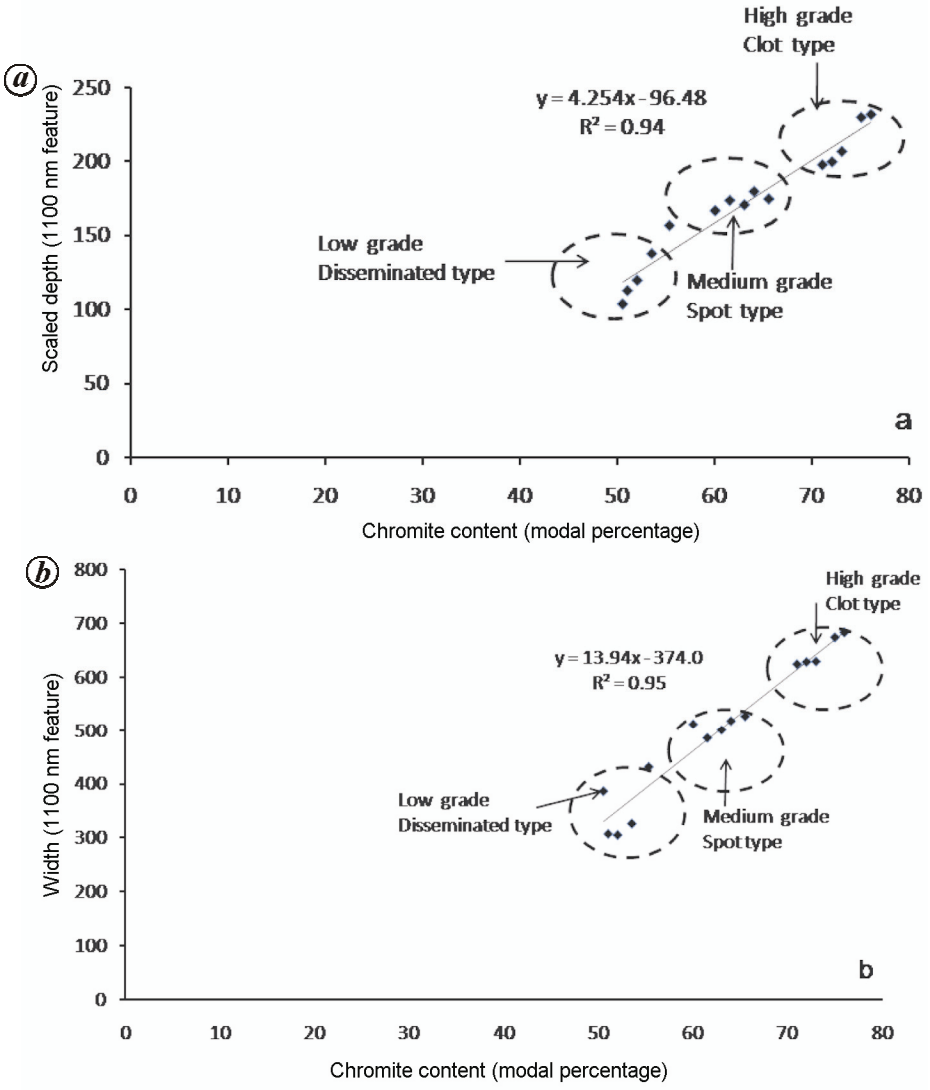

Figure 7. ***a***, Regression plot of depth of spectral feature at 1100 nm and modal abundance of chromite (depth is multiplied by 1000 to show contrast in interger) in chromitite samples of three textural varieties. ***b***, Regression plot of width of spectral feature at 1100 nm and modal abundance of chromite in chromitite samples of three textural varieties.

chromitite samples of different textures after deriving the above spectrometric parameters from the normalized spectra of the pulverized sample. Interestingly, we found that both depth and width had positive correlation with the chromite mineral content of the sample (Figures 7 *a* and *b*). Width had a correlation value of 0.95 while depth had a correlation value of 0.94 with abundance (Figures 7 *a* and *b*). Although grain size ranges of constituent minerals of chromitite of different textures were very close in the consolidated rock, the effect of intimate mixing in measurements of quantitative parameters of the absorption feature was further reduced in the pulverized samples of each textural variety (five sample for each texture) used to relate modal abundances of chromite with spectrometric parameters. As discussed in Table 3, the feature at 1100 nm was due to Fe^{2+} in chromite grains. EPMA data of chromite and chlorite grains of each texture were used to relate Fe^{2+} abundance with the absorption feature (Table 2). However, Fe^{2+} was also present in chlorite mineral. But the abundance of Fe in chlorite was very low (less than 5%). Further, modal abundances of chlorite itself were low in these samples (varied from 20% to 40% in different textures) (Table 1). Therefore, contribution of Fe^{2+} of chlorite to the spectrometric parameters around 1100 nm would be multiplicatively negligible. High oxidation of chromitite was regarded responsible for shifting the Fe^{2+} absorption feature beyond 1000 nm towards higher wavelength[17,39]. This was due to shift in Fe^{2+} from the tetrahedral site to the octahedral site in the structure of chromite minerals of chromitite samples[17,39]. A further concomitant absorption feature due to Fe^{3+} was also noticed in chromitite spectra (specially distinct in the spectra of spot type texture) at 550–600 nm when abundance of Fe^{3+} increased[17,40] (Table 2). Hence, width and depth

Table 3. Description of major spectral features of chromitite

Rock	Central wavelength of spectral feature	Dominant minerals	Atomic process involved
Chromitite	550 nm (I–C)	Chromite and chlorite	Absorption of incident energy caused due to charge transfer process in Fe^{3+} (present in chromite). It is prominent in the spotted texture chromitite sample as it had Fe^{3+} abundance. In the spectra of clot type, features due to Fe^{3+} and Fe^{2+} were welded to make a broad feature.
	1100 nm (II–C)		Absorption of incident energy caused due to crystal field process in Fe^{2+} (present in chromite). This feature is common to all the textures.
	1400 nm (III–C)		Absorption of incident energy caused due to OH bond stretching vibration (OH in chlorite). It is common in spotted and disseminated textured chromitite.
	1800–1950 nm (IV–C)		Absorption of incident energy caused due to bending of OH for free water molecule in mineral structure. It is common in all the textures. OH feature has central wavelength at 1900 nm whereas Fe^{2+} feature had absorption at 1800 nm (approximate).
	2200 nm (V–C)		Al–OH bond vibration in chlorite. This may be due to the presence of Al on octahedral place. Similar Al-OH feature was reported in chlorite mineral[37]. It is observed in clot type chromitite sample. Fe^{2+} in chromitite was responsible for this feature[15].
	2300 nm (VI–C)		Mg–OH bond vibration in chlorite[37].

of this feature can be used as a relative indicator of abundance of chromite mineral as the 1100 nm feature was attributed to Fe^{2+} of chromite mineral in chromitite.

Conclusions

Based on the results of the mineralogical analysis of rock spectra of chromitite samples of three different textural variants and the spectra of few samples of same texture, we have derived the following conclusions:

- Chromitite spectra are sensitive to textural variations. These textural variations are in turn attributed to the variation in modal abundances of chromite and chlorite and their mutual arrangements in the rock fabric (Figures 3 and 4 and Table 1). Therefore, reflectance spectroscopy has a potential role in estimating the relative grade of chromitite.
- Spectral features of chromitite are influenced by the absorption feature due to electronic transition process in Fe^{3+} ion and crystal field effect in Fe^{2+} occurring within chromitite[17,39]. Spectral features around 1400 nm, 1900 nm and 2300 nm are due to chlorite, while spectral features around 550 nm and 1100 nm are governed by chromite (Table 3).
- There are few spectral features which are common in all three textural variants of chromitite (Figure 4). These spectral features have their wavelength of absorption at 1100 nm and also within the spectral range of 1800–1900 nm. The spectral feature at 1900 nm is attributed to the vibration in the bond of H_2O molecule present in chlorite. However, the broader spectral feature around 1800–1900 nm for clot type chromitite was not only due to chlorite, but was also broadened due to Fe^{2+} as it also has absorption at 1800 nm (Figure 4 and Table 3). High oxidation of chromitite resulted in shifting the Fe^{2+} absorption feature beyond 1000 nm. This was due to shift in Fe^{2+} from the tetrahedral site to octahedral site in the structure of chromite minerals of chromitite samples[17,39].
- A further concomitant absorption feature due to Fe^{3+} is also noticed in chromitite spectra (specially distinct in the spectra of spot type texture) at 550–600 nm when abundance of Fe^{3+} increased[17,28] (Table 2). On the other hand, all the absorption features due to Fe^{3+} and Fe^{2+} are wielded to derive a large absorption feature in the spectra of clot type chromitite (Figure 6 *a*).
- It is also observed that the spectral feature at 1100 nm was common to the three textural variants of chromitite, but width and depth of the spectral feature were variable in different textural varieties but same (i.e. very close) for samples of the same texture (Figure 5 *c* and Table 1). Width has a correlation value of 0.95 while depth has a correlation value of 0.94 with chromite abundance in chromitite (Figure 7).

1. Hunt, G. R. and Salisbury, J. W., Visible and near-infrared spectra of minerals and rocks: II. Carbonates. *Mod. Geol.*, 1971, **2**, 23–30.
2. Clark, R. N. and Roush, T. L., Reflectance spectroscopy quantitative analysis techniques for remote sensing applications. *J. Geophys. Res.*, 1984, **89**(B7), 6329–6340.
3. Clark, R. N., Spectroscopy of rocks and minerals, and principles of spectroscopy. USGS spectral laboratory; http://speclab.cr.usgs.gov/spectral-lib.html (accessed 7 December 2011).

4. Clark, R. N., King, T. V. V., Klejwa, M. and Swaze, G. A., High spectral resolution reflectance spectroscopy of minerals. *J. Geophys. Res.*, 1990, **95**(B8), 12653–12680.
5. Cloutis, E. A., Hyperspectral geological remote sensing: evaluation of analytical techniques. *Int. J. Remote Sensing*, 1996, **17**(12), 2215–2242.
6. Clark, R. N., Swayze, G. A., Heidebrecht, K., Green, R. O. and Goetz, A. F. H., Calibration to surface reflectance of terrestrial imaging spectrometry data: comparison of methods, summaries of the fifth annual JPL airborne geosciences workshop. Jet Propulsion Laboratory Special Publication, 1995, pp. 41–42.
7. Guha, A., Chakraborty, D., Ekka, A. B., Pramanik, K. and Chatterjee, S., Spectroscopic study of rocks of Hutti-Maski Schist Belt, Karnataka. *J. Geol. Soc. India*, 2012, **79**, 335–344.
8. Guha, A., Rao, A., Ravi, S., Vinod Kumar, K. and Dhananjaya Rao, E. N., Analysis of the potentials of kimberlite rock spectra as spectral end member – a case study using kimberlite rock spectra from the Narayanpet kimberlite Field (NKF), Andhra Pradesh. *Curr. Sci.*, 2012, **103**(9), 1096–1104.
9. Carli, C. and Sgavetti, M., Spectral characteristics of rocks: effects of composition and texture and implications for the interpretation of planet surface compositions. *Icarus*, 2011, **211**(2), 1034–1048.
10. Dennis, K. M., Spectral properties (0.4 to 25 microns) of selected rocks associated with disseminated gold and silver deposits in Nevada and Idaho. *J. Geophys. Res.: Solid Earth*, 1986, **91**(B1), 2156–2202.
11. Guha, A., Vinod Kumar, K., Ravi, S. and Dhanamjaya Rao, S., Reflectance spectroscopy of kimberlites – in parts of Dharwar Craton, India. *Arabian J. Geosci*., 2015, **8**(11), 9373–9388.
12. Khan, S. D. and Mahmood, K., The application of remote sensing techniques to the study of ophiolites. *Earth Sci. Rev.*, 2008, **89**, 135–143.
13. Khan, S. D., Mahmood, K. and Casey, J. F., Mapping of Muslim Bagh ophiolite complex (Pakistan) using new remote sensing and field data. *J. Asian Earth Sci.*, 2007, **30**, 333–343.
14. Pournamdari, M., Hashim, M. and Pour, A. B., Spectral transformation of ASTER and Landsat TM bands for lithological mapping of *Soghan ophiolite* complex, south Iran. *Adv. Space Res.*, 2014, **54**, 694–709.
15. Rajendran, S. *et al.*, ASTER detection of chromite bearing mineralized zones in Semail Ophiolite Massifs of the northern Oman Mountains: exploration strategy. *Ore Geol. Rev.*, 2012, **44**, 121–135.
16. van der Meer, F., Analysis of spectral absorption features in hyperspectral imagery. *Int. J. Appl. Earth Observ. Geoinfor.*, 2004, **5**, 55–68.
17. Tangestani, M. H., Jaffari, L., Vincent, R. K. and Maruthi Sridhar, B. B., Spectral characterization and ASTER-based lithological mapping of an ophiolite complex: a case study from Neyriz ophiolite, SW Iran. *Remote Sensing Environ.*, 2011, **115**, 2243–2254.
18. Mukherjee, R., Mondal, S. K., Rosing, M. T. and Frei, R., Compositional variations in the *Mesoarchean chromites* of the Nuggihalli schist belt, Western Dharwar Craton (India): potential parental melts and implications for tectonic setting. *Lithos*, 2010, **160**, 865–885.
19. ASD, I., Field spec specification, 2012; www.asdi.com.
20. Blom, R. G., Abrams, M. J. and Adams, H. G., Spectral reflectance and discrimination of plutonic rocks in the 0.45–2.45 μm region. *J. Geophys. Res.*, 1980, **85**(B5), 2156–2202.
21. Walter, L. S. and Salisbury, J. W., Spectral characterization of igneous rocks in the 8–12 μm region. *J. Geophys. Res.-Solid Earth*, 1989, **94**(B7), 2156–2202.
22. Cloutis, E. A., Sunshine, J. M. and Morris, R. V., Spectral reflectance-compositional properties of spinels and chromites: implications for planetary remote sensing and geothermometry. *Meteor. Planet. Sci.*, 2004, **39**(4), 545–565.
23. Mitra, S. and Bidyananda, M., Evaluation of metallogenic potential of the Nuggihalli greenstone belt, South India. *C. R. Geosci.*, 2003, **335**(2), 185–192.
24. Ramakrishnan, M., Precambrian mafic magmatism in the western Dharwar craton, Southern India. *J. Geol. Soc. India*, 2009, **73**, 101–116.
25. Radhakrishna, B. P. and Vaidyanathan, R., Geology of Karnataka, Geological Society of India, Bangalore, 1994, p. 298.
26. Devaraju, T. C., Viljoen, R. P., Sawkar, R. H. and Sudhakara, T. L., Mafic and ultramafic magmatism and associated mineralization in the Dharwar craton, southern India. *J. Geol. Soc. India*, 2009, **73**, 73–100.
27. Droop, G. T. R., A general equation for estimating Fe^{3+} concentrations in ferromagnesian silicates and oxides from microprobe analysis, using stoichiometric criteria. *Mineral. Mag.*, 2011, **51**, 431–435.
28. Ghosh, B. and Konar, R., Chromites from metaanorthosites, Sitampundi layered igneous complex, Tamil Nadu, southern India. *J. Asian Earth Sci.*, 2011, **42**, 1394–1402.
29. Milton, E. J., Schaepman, M. E., Anderson, K., Kneubahler, M. and Fox, N., Progress in field spectroscopy. *Remote Sensing Environ.*, 2009, **113**, S92–S109.
30. Baldridge, A. M., Hook, S. J., Grove, C. I. and Rivera, G., The ASTER spectral library version 2.0. *Remote Sensing Environ.*, 2009, **113**, 711–715.
31. Nicodemus, F. F., Richmond, J. C., Hsia, J. J., GIinsberg, I. W. and Limperis, T. L., Geometrical considerations and nomenclature for reflectance In *National Bureau of Standards Monograph* (ed. Office, D. C. U. S. G.), Washington, 1977, p. 20402.
32. Biggar, S. F., Labed, J., Santer, R. P. and Slater, P. N., Laboratory calibration of field reflectance panels. In Proceedings of SPIE – The International Society for Optical Engineering (ed. Slater, P. N.), Orlando, Florida, 1988, pp. 232–240.
33. Bruegge, C. J., Chrien, N. and Haner, D., A spectralon BRF database for MISR calibration applications. *Remote Sensing Environ.*, 2001, **76**, 354–366.
34. Crowley, J. K., Visible and near-infrared spectra of carbonate rocks reflectance variations related to petrographic texture and impurities. *J. Geophys. Res*., 1986, **91**(B5), 5001–5012.
35. Okada, K. and Iwashita, A., Hyper-multispectral image analysis based on waveform characteristics of spectral curve. *Adv. Space Res.*, 1992, **12**, 433–442.
36. van der Meer, F. D., Basic physics of spectrometry. In *Imaging Spectrometry: Basic Principles and Prospective Applications* (eds van der Meer, F. D. and de Jong, S. M.), Springer, Dordrecht, 2006, pp. 3–16.
37. Trude, K. V. V. and Clark, R. N., Spectral characteristics of chlorites and Mg-serpentines using high-resolution reflectance spectroscopy. *J. Geophys. Res.: Solid Earth*, 1989, **B10**, 13997–14008.
38. Jafri, S. H., Khan, N., Ahmad, S. M. and Saxena, R., Geology and Geochemistry of Nuggihalli Schist belt, Dharwar craton, Karnataka, India. In *Precambrian of South India* (eds Naqvi, S. M. and Rogers, J. J. W.), Memoir Geological Society of India, 1983, vol. 4, pp. 110–120.

ACKNOWLEDGEMENTS. We thank the Director, National Remote Sensing Centre (NRSC) for his support and overall guidance. We also thank the Deputy Director, RSAA NRSC for providing facilities to carry out this work. The field work was supported with financial grant received from UGC DRS (2013–2018).

Received 25 November 2016; revised accepted 6 November 2017

doi: 10.18520/cs/v114/i08/1721-1731